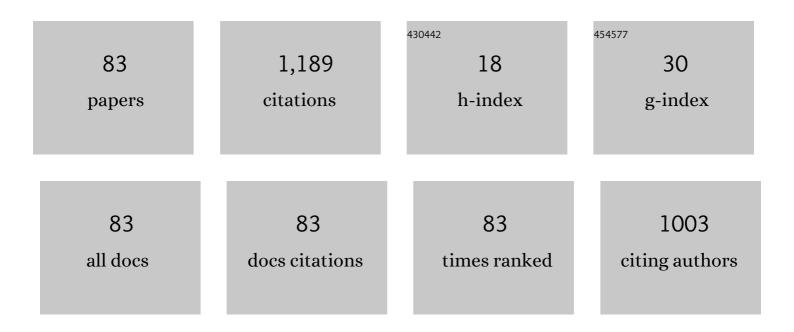


List of Publications by Year in descending order

Source: https://exaly.com/author-pdf/155039/publications.pdf Version: 2024-02-01



#	Article	IF	CITATIONS
1	Triple-band tunable perfect terahertz metamaterial absorber with liquid crystal. Optics Express, 2017, 25, 32280.	1.7	86
2	Ultrasensitive Tunable Terahertz Sensor With Graphene Plasmonic Grating. Journal of Lightwave Technology, 2019, 37, 1103-1112.	2.7	71
3	Liquid crystal terahertz modulator with plasmon-induced transparency metamaterial. Optics Express, 2018, 26, 5769.	1.7	68
4	Ultra-large electric field–induced strain in potassium sodium niobate crystals. Science Advances, 2020, 6, eaay5979.	4.7	53
5	Metalens for Generating a Customized Vectorial Focal Curve. Nano Letters, 2021, 21, 2081-2087.	4.5	51
6	Multi-foci metalens for terahertz polarization detection. Optics Letters, 2020, 45, 3506.	1.7	42
7	Diode-pumped continuous wave and passively Q-switched Tm,Ho:LLF laser at 2 µm. Optics Express, 2013, 21, 12629.	1.7	37
8	All-optical switch and limiter based on nonlinear polarization in Mach–Zehnder interferometer coupled with a polarization-maintaining fiber-ring resonator. Optics Communications, 2006, 260, 318-323.	1.0	35
9	Field-driven electro-optic dynamics of polar nanoregions in nanodisordered KTa1â^' <i>x</i> Nb <i>x</i> O3 crystal. Applied Physics Letters, 2017, 111, .	1.5	35
10	Controlling plasmon-induced transparency of graphene metamolecules with external magnetic field. Optics Express, 2015, 23, 12524.	1.7	34
11	A novel strategy for markedly enhancing the red upconversion emission in Er ³⁺ /Tm ³⁺ cooperated nanoparticles. Journal of Materials Chemistry C, 2018, 6, 7533-7540.	2.7	33
12	Diode-pumped actively Q-switched Tm, Ho:GdVO_4/BaWO_4intracavity Raman laser at 2533Ânm. Optics Letters, 2013, 38, 1206.	1.7	29
13	Strain-Gradient-Controlled Disorder Dynamics in Chemically Substituted Ferroelectrics. Physical Review Applied, 2019, 11, .	1.5	28
14	Super terahertz phase shifter achieving high transmission and large modulation depth. Optics Letters, 2020, 45, 2834.	1.7	26
15	Heat generation and thermal lensing in end-pumped Tm,Ho : YLF laser crystals. Journal Physics D: Applied Physics, 2007, 40, 6930-6935.	1.3	24
16	Highly Birefringent Single-Mode Suspended-Core Fiber in Terahertz Regime. Journal of Lightwave Technology, 2018, 36, 3242-3248.	2.7	22
17	Diode-pumped actively Q-switched Tm:YAP/BaWO_4 intracavity Raman laser. Optics Express, 2015, 23, 10075.	1.7	21
18	Extremely high Q-factor terahertz metasurface using reconstructive coherent mode resonance. Optics Express, 2021, 29, 7015.	1.7	21

#	Article	IF	CITATIONS
19	Investigation of Hot Carrier Cooling Dynamics in Monolayer MoS ₂ . Journal of Physical Chemistry Letters, 2021, 12, 861-868.	2.1	20
20	Orthogonally polarized dual-wavelength single-longitudinal-mode Tm,Ho:LLF laser. Optics Express, 2013, 21, 22699.	1.7	19
21	72-fs Er-doped Mamyshev Oscillator. Journal of Lightwave Technology, 2022, 40, 2123-2127.	2.7	19
22	Ultrafast, low power, and highly stable all-optical switch in MZI with two-arm-sharing nonlinear ring resonator. Optics Communications, 2005, 256, 319-325.	1.0	18
23	An ultrahigh <i>Q</i> -factor dual-band terahertz perfect absorber with a dielectric grating slit waveguide for sensing. Journal Physics D: Applied Physics, 2020, 53, 235103.	1.3	18
24	Diode-end-pumped continuously tunable single frequency Tm, Ho:LLF laser at 206  μm. Applied Optics, 2014, 53, 1488.	0.9	17
25	Efficient terahertz polarization conversion with hybrid coupling of chiral metamaterial. Optics Letters, 2020, 45, 1276.	1.7	17
26	Bandgap separation and optical switching in nonlinear chiral photonic crystal with layered structure. IEEE Photonics Technology Letters, 2006, 18, 1261-1263.	1.3	16
27	Broadband single-polarization optical fiber based on surface plasmon resonance. Applied Optics, 2020, 59, 779.	0.9	16
28	Energy transfer enhanced laser cooling in Ho^3+ and Tm^3+-codoped lithium yttrium fluoride. Journal of the Optical Society of America B: Optical Physics, 2013, 30, 939.	0.9	15
29	Recent research progress of Mamyshev oscillator for high energy and ultrashort pulse generation. Optical Fiber Technology, 2021, 67, 102691.	1.4	15
30	Laser diode end-pumped passively Q-switched Tm,Ho:YLF laser with Cr:ZnS as a saturable absorber. Optics Communications, 2012, 285, 2122-2127.	1.0	14
31	The influence of side-coupled quantum dots on thermoelectric effect of parallel-coupled double quantum dot system. Physica B: Condensed Matter, 2018, 545, 377-382.	1.3	14
32	Full telecomband covered half-wave meta-reflectarray for efficient circular polarization conversion. Optics Communications, 2018, 427, 469-476.	1.0	14
33	Reconstructing subwavelength resolution terahertz holographic images. Optics Express, 2022, 30, 7137.	1.7	14
34	Ultra-broadband perfect terahertz absorber with periodic-conductivity graphene metasurface. Optics and Laser Technology, 2022, 154, 108297.	2.2	14
35	The effects of energy transfer upconversion on end-pumpedQ-switched Tm, Ho : YLF lasers. Journal Physics D: Applied Physics, 2009, 42, 025107.	1.3	13
36	Mechanical control of terahertz plasmon-induced transparency in single/double-layer stretchable metamaterial. Journal Physics D: Applied Physics, 2021, 54, 035101.	1.3	13

#	Article	IF	CITATIONS
37	A dual-core fiber for tunable polarization splitters in the terahertz regime. Optics Communications, 2021, 480, 126463.	1.0	11
38	Impact of dipolar clusters on electro-optic effects in KTa ₁₋ _x Nb _x O ₃ crystal. Optics Letters, 2018, 43, 5009.	1.7	11
39	A theoretical study of intrinsic optical bistability dynamics in Tm3+/Yb3+codoped systems with an upconversion avalanche mechanism. Journal of Optics, 2009, 11, 105203.	1.5	9
40	Formation mechanism of optical bistability in end-pumped quasi-three-level Tm, Ho:YLF lasers. Journal of the Optical Society of America B: Optical Physics, 2009, 26, 2434.	0.9	9
41	All-Polarization-Maintaining Passively Mode-Locked Erbium-Doped Fiber Laser Based on a WDM-Isolator-Tap Hybrid Device. Journal of Russian Laser Research, 2021, 42, 82-86.	0.3	9
42	Dual-band terahertz switch with stretchable Bloch-mode metasurface. New Journal of Physics, 2020, 22, 113008.	1.2	9
43	Ultrafast carrier dynamics in double perovskite Cs ₂ AgBiBr ₆ nanocrystals. Applied Physics Express, 2020, 13, 121003.	1.1	9
44	ReSe2 passively Q-switched Nd:Y3Al5 O12 laser with near repetition rate limit of microsecond pulse output. Optics Communications, 2019, 445, 165-170.	1.0	8
45	Graphene/liquid crystal hybrid tuning terahertz perfect absorber. Applied Optics, 2019, 58, 9406.	0.9	8
46	Laser-driven blackbody radiator with bistability. Applied Physics B: Lasers and Optics, 2014, 116, 867-873.	1.1	7
47	Double D-shaped hole optical fiber coated with graphene as a polarizer. Applied Optics, 2018, 57, 7659.	0.9	7
48	Watt-Level Continuous-Wave Mode-Locked Nd:YVO ₄ Laser With ReSe ₂ Saturable Absorber. IEEE Photonics Journal, 2020, 12, 1-10.	1.0	6
49	A modified dual-core THz fiber polarization splitter with four subwavelength tubes. Optik, 2021, 225, 165862.	1.4	6
50	Controllable Terahertz Switch Using Toroidal Dipolar Mode of a Metamaterial. Plasmonics, 2021, 16, 933-938.	1.8	6
51	Mode-locking operation of an Er-doped fiber laser with (PEA) ₂ (CsPbBr ₃) _{<i>n</i>â^`1} PbBr ₄ perovskite saturable absorbers. Journal of Materials Chemistry C, 2022, 10, 7504-7510.	2.7	6
52	Numerical analysis of intrinsic bistability and chromatic switching in Tm3+single-doped systems under photon avalanche pumping scheme. Journal Physics D: Applied Physics, 2008, 41, 195105.	1.3	5
53	Intrinsic Bistability and Critical Slowing in Tm ³⁺ /Yb ³⁺ Codoped Laser Crystal with the Photon Avalanche Mechanism. Chinese Physics Letters, 2009, 26, 064216.	1.3	5
54	Suppression of energy transfer from Er3+ to OHâ^' in Er3+ highly doped zirconia. Optics Communications, 2013, 287, 228-233.	1.0	5

#	Article	IF	CITATIONS
55	Two-core single-polarization optical fiber with a large hollow coated bimetallic layer. Applied Optics, 2018, 57, 2446.	0.9	5
56	Color tuning in a compact core-shell nanocrystal based on intense and high-purity green and red photon upconversion. Optics Letters, 2021, 46, 900.	1.7	5
57	Tunable terahertz slow light of a cavity-integrated guided-mode resonance grating. Journal of the Optical Society of America B: Optical Physics, 2021, 38, 1710.	0.9	5
58	A Novel All-Optical Switch in a Double-Loop Sagnac Ring Coupled with a Nonlinear Ring Resonator. Chinese Physics Letters, 2004, 21, 2205-2208.	1.3	4
59	Optical bistability and Fano-like resonance transmission in a ring cavity-coupled Michelson interferometer. Journal of Optics, 2008, 10, 075305.	1.5	4
60	Electron transport through a linear tri-quantum-dot molecule Aharonov-Bohm interference. Physica B: Condensed Matter, 2017, 521, 148-152.	1.3	4
61	Tunable plasmon-induced transparency with a dielectric grating-coupled graphene structure for slowing terahertz waves. Applied Optics, 2020, 59, 7179.	0.9	4
62	Tunable terahertz group slowing effect with plasmon-induced transparency metamaterial. Applied Optics, 2022, 61, 3218.	0.9	4
63	Photon-assisted electronic and spin transport through two T-shaped three-quantum-dot molecules embedded in an Aharonov–Bohm interferometer. Chinese Physics B, 2017, 26, 117302.	0.7	3
64	Cooling and diffusion characteristics of a hot carrier in the monolayer WS ₂ . Optics Express, 2021, 29, 7736.	1.7	3
65	Electron transport through a two-terminal Aharonov-Bohm interferometer coupled with linear di-quantum dot molecules. Wuli Xuebao/Acta Physica Sinica, 2015, 64, 207304.	0.2	3
66	Investigation of thermal effects in a diode end-pumped Tm,Ho:YLF solid state laser. , 2010, , .		2
67	All-optical switch with low threshold over a wide wavelength range by use of a Mach–Zehnder racetrack resonator. Journal of Optics, 2007, 9, 848-853.	1.5	1
68	<title>Influence of energy-transfer up-conversion on diode-end-pumped Q-switched Tm,Ho:YLF
lasers</title> . , 2007, , .		1
69	Bistable upconversion emission in Yb-sensitized Tm:ZrO2 nanophosphors at room temperature. Journal of Nonlinear Optical Physics and Materials, 2016, 25, 1650009.	1.1	1
70	A modified large mode-field area fiber with managing chromatic dispersion. Optik, 2020, 208, 164104.	1.4	1
71	A modified single-polarization THz fiber with epsilon-near-zero (ENZ) material. Results in Optics, 2020, 1, 100034.	0.9	1
72	Theoretical and experimental investigation of thermal effect in end-pumped Tm,Ho:YLF lasers. Proceedings of SPIE, 2007, , .	0.8	0

#	Article	IF	CITATIONS
73	Optical bistability in an end-pumped Tm,Ho:YLF laser at room temperature. , 2007, , .		0
74	Tunable bistability and asymmetric line shape in ring cavity-coupled Michelson interferometer. Proceedings of SPIE, 2007, , .	0.8	0
75	Intrinsic optical bistability in Tm-doped laser crystal pumped at 648nm avalanche wavelength. , 2007, , .		0
76	Investigation of thermal effects in longitudinally diode-pumped Tm,Ho:YLF lasers. Proceedings of SPIE, 2007, , .	0.8	0
77	Bistable chromatic switching in 648 nm laser pumped Tm-doped crystal. , 2007, , .		0
78	<title>Resonator-enhanced low power all-optical switch with a nonlinear ratio-variable
coupler</title> . , 2007, , .		0
79	Bistable performances of diode-end-pumped quasi-three-level Tm,Ho:YLF lasers. Optics Communications, 2010, 283, 1086-1089.	1.0	0
80	Enhanced laser cooling of Tm-doped solids by upconversion pumping. , 2013, , .		0
81	Bistability of laser-induced thermal radiation in rare earth doped solids. , 2013, , .		0
82	Evaluation of Anti-Stokes Superradiance Cooling Thulium Doped Solids. , 2014, , .		0
83	A single-longitudinal-mode Tm, Ho:YAG laser. , 2017, , .		Ο